Research Article | Vol. 10, No. 12 / 1 December 2020 / Optical Materials Express 3403
Optical Materials EXPRESS

Comparison of different in situ optical temperature probing techniques for cryogenic Yb:YLF

UMIT DEMIRBAS,[1,2,*] JELTO THESINGA,[1] MARTIN KELLERT,[1] FRANZ X. KÄRTNER,[1,3] AND MIKHAIL PERGAMENT[1]

[1]Center for Free-Electron Laser Science, Deutsches Elektronen-Synchrotron DESY, Luruper Chaussee 149, 22761 Hamburg, Germany
[2]Laser Technology Laboratory, Antalya Bilim University, 07190 Dosemealti, Antalya, Turkey
[3]Physis Department and The Hamburg Centre for Ultrafast Imaging, University of Hamburg, Luruper Chaussee 149, 22761 Hamburg, Germany
*uemit.demirbas@cfel.de

Abstract: We present, what is to our knowledge, the first detailed set of experiments comparing different in situ optical temperature estimation methods for Yb:YLF ($Yb:LiYF_4$) crystals used in cryogenic laser applications. The proposed temperature estimation methods are based on the temperature dependence of emission spectra of Yb:YLF in E//c axis, and looks at either the variation of the spectral intensity ratio of different wavelengths, or to the full-width half-maximum (FWHM) of the emission lines, or to the overall absolute integrated spectral change with respect to a reference temperature (also known as Differential Luminescence Thermometry: DLT). We have shown that by using the DLT method we can estimate the temperature of Yb:YLF crystals in the 78-300 K range with an accuracy better than ±1 K. The other methods work well in the 78-150 K range, and provide a fast temperature estimation with ±2 K accuracy. The benefit of the proposed technique has been demonstrated via evaluation of thermal contact quality of different Yb:YLF crystals, where we have seen that, a temperature estimation accuracy of ±5 K is feasible even for samples under nonhomogeneous thermal load. We hope the findings presented in this work to be useful to laser engineers and scientists working with cryogenic Yb:YLF systems.

© 2020 Optical Society of America under the terms of the OSA Open Access Publishing Agreement

1. Introduction

Since its first lasing demonstration in 2001 by Kawanaka *et al.* [1], Yb:YLF ($Yb:LiYF_4$) has been getting frequent attention of laser scientists as a versatile broadband laser gain material [2–7]. As a very rare property among the known laser materials, the emission cross section of Yb:YLF stays broad (FWHM:∼10 nm) even at cryogenic temperatures [1,8]. Besides the broad gain bandwidth, cryogenic temperatures also provide the usual improvements in gain cross section, and thermal material parameters [8–11]. As a result, operating Yb:YLF at cryogenic temperatures provides 2-3 orders of magnitude higher average powers compared to room-temperature operation [12–16]. Despite this progress, unfortunately, to our knowledge, important laser related material properties such as the polarizability difference parameter and the photoelastic parameters for YLF are not known [17–20]. Hence, a detailed understanding of thermal effects and the resulting thermal lens is lacking in Yb:YLF, especially at cryogenic temperatures.

As a first step towards a better understanding of the thermal effects in Yb:YLF, we study different methods that could be used in probing the temperature of Yb:YLF crystals at cryogenic temperatures. For this purpose, we have first investigated the temperature dependence of several parameters such as upper state fluorescence lifetime, absorption and emission. Our initial analysis has shown that, among the investigated parameters, the variation of emission spectra with temperature in the E//c axis of Yb:YLF has the steepest slope of change with temperature,

#411331 https://doi.org/10.1364/OME.411331
Journal © 2020 Received 28 Sep 2020; revised 14 Nov 2020; accepted 19 Nov 2020; published 30 Nov 2020

Optical Materials EXPRESS

especially in the 990-1000 nm spectral range, and it could potentially provide a means for minimal measurement uncertainty.

Hence, using the E//c emission of Yb:YLF gain media, we have developed/used several techniques for temperature estimation that are based on: (i) measuring the intensity ratios in different spectral regions of emission, (ii) measuring the FWHM of emission lines, and (iii) by looking at the spectral variation of the whole emission spectra. The last technique, which is known as Differential Luminescence Thermometry (DLT), has already been successfully used in estimating the temperature of Yb:YLF samples in cryogenic optical refrigeration experiments [21–27]. However, these studies took the room-temperature spectra as a reference while looking at the spectral change and in our case the 78 K spectrum is referenced, since for laser applications, our focus is in estimating temperatures in the 78-150 K range. Moreover, to our knowledge, a detailed analysis of the DLT technique usage in Yb:YLF and its error margins is not studied yet. H. Furuse *et al*. have used intensity ratios at two emission wavelength for temperature estimation of cryogenic Yb:YAG laser crystals [28], and H. Chi extended the method for 3-dimensional temperature mapping that could be used for accurate temperature prediction even under lasing/amplification conditions [29]. However, to our knowledge, similar studies have not yet been performed for cryogenic Yb:YLF laser gain media.

In this study, we are presenting a first set of detailed experiments, where we propose different temperature estimation methods for Yb:YLF crystals and investigate pros and cons of each technique. In our work, we have seen that, if the reference data is taken carefully, the DLT method could be used to estimate the temperature of Yb:YLF within ±1 K accuracy in the 78-300 K range. We have further shown that by looking at the ratio of intensities or by looking at the FWHM of the emission line, a fast real-time temperature estimation with an accuracy of ±2 K could also be made in the 78-150 K range. A detailed comparison of different methods and the experimental challenges for accurate temperature measurements will also be discussed. As a sample case, we will present temperature measurements of several indium bonded Yb:YLF laser crystals cooled by liquid nitrogen, where the capability of the method in analyzing the thermal contact quality of the samples will be shown.

The paper is organized as follows: Section 2 presents the experimental setup, and Section 3 describes the different techniques that were employed in temperature estimation of Yb:YLF. In Section 4, we analyze and discuss the temperature estimation accuracy of different methods. Section 5 presents sample temperature measurements of Yb:YLF laser crystals under thermal load. Finally, in Section 6, we conclude with a brief discussion.

2. Experimental methodology

As mentioned earlier, the temperature estimation methods we propose/use in this study is based on the measured variation of emission spectra of Yb:YLF in c-axis with temperature. Several Yb:YLF crystals with Yb-doping of 0.5% and 1% were available for the experiments. The crystals have 20-mm long Yb-doped sections and 3-mm long un-doped end cap diffusion bonded sections on both ends (total crystal length: 26 mm, height: 10 mm, width 15 mm. They are indium soldered from the top side to a multi-stage pyramidal cold head, which was cooled to cryogenic temperatures by boiling liquid nitrogen (Figs. 1(a)–1(b)). Several thermal sensors connected to the cold head near the crystal enabled real time measurement of cold head temperature with ±0.1 K accuracy. For temperature dependent emission measurements, the dewar cooling cycle is used, as employed in [30]. The dewar is first filled with some limited amount of liquid nitrogen, and thermal equilibrium is reached at 78 K. Afterwards, once the nitrogen is evaporated, the bulky dewar interior mass including the crystal and the cold head heats up very slowly in 6-7 hours. During this long cooling process, the crystals and the cold head is in thermal equilibrium, and the crystal temperature could be accurately measured using the thermal sensors. Care is taken during

Optical Materials EXPRESS

the emission measurements not to heat up the crystal by minimizing the power of the excitation beam.

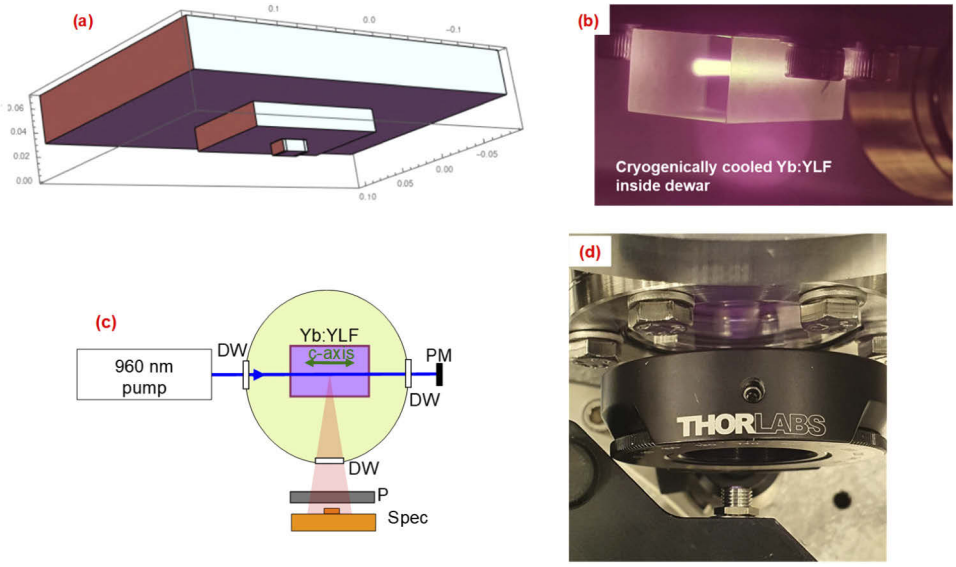

Fig. 1. (a) Yb:YLF crystal indium soldered to the copper alloy heat sink. The top part of the heat sink is in direct contact with boiling liquid nitrogen. (b) A photo of the Yb:YLF crystals under cw excitation at 960 nm. The crystal dimensions have been 10 mm x 15 mm x 26 mm, and the pump beam had a dimeter of around 2.55 mm. (c) A simple schematic of the temperature measurement setup. DW: Dewar window, P: Polarizer, PM: Power meter, Spec: Spectrometer. Dimensions are not to scale. (d) A photo of the temperature measurement system: dewar side window, polarizer and the entrance of the spectrometer are partly visible in the photo.

A fiber-coupled, 960 nm laser diode with an M^2 of around 220 was used as the excitation source. The pump light is collimated and imaged inside the gain medium using a set of appropriate lenses, resulting in a flattop beam profile with a beam diameter of 2.08 mm at the center of the crystal (root mean square value of the beam diameter along the crystal length is 2.55 mm). This beam size is also what was used in earlier laser experiments [13,16] and represents a reasonable laser pumping geometry. In emission measurements, Yb:YLF crystals are excited with 500 µs long pump pulses with 1.5 kW of peak power at 1 Hz repetition rate. Due to the low duty cycle employed, the average absorbed pump power was below 0.5 W in these measurements, and hence the heat load on the crystal is very limited (we estimate an average temperature rise below 0.1 K at this pump power). The reference emission spectra were measured at a 90° angle to the pump propagation direction via windows either at the side or at the bottom of the dewars (Figs. 1(c)–1(d)). We have concentrated our attention to the emission in the c-axis and a thinfilm polarizer (Thorlabs LPNIRE100-B) was used for selecting the emission in the relevant axis. The Ocean Optics HR4000 spectrometer used in the measurements was based on a 3648 pixel CCD array (Toshiba TCD1304AP). The spectrometer contained a very narrow entrance slit of 5µm, and it was custom-modified to provide a spectral resolution of 0.1 nm in the 900-1060 nm range. The cylindrical metallic entrance at the spectrometer input prevented entrance of stray light into the system and provided some directionality. In the experiments, the spectrometer entrance was aligned to look at the central portion of the crystal. The distance between the crystal and spectrometer input was around 15 cm and due to the large emission intensity a strong emission signal could be acquired even without using any imaging element. We have used the spectrometer

Optical Materials EXPRESS

in free-space configuration while taking the data that we will present in this study. However, in our experiments we have seen that fiber coupling could also provide similar performance (a 200 μm core multimode fiber with an NA of 0.22 was used alternatively: M200L02S-B from Thorlabs). The overall spectral response of the measurement system (CCD array, grating, film polarizer) was corrected using the spectral response curves provided by the companies and our spectral response correction was also confirmed with measurements performed with broadband emission sources with known spectral distribution. We estimate fluorescence intensity accuracy better than ±20% in our measurements. We have focused our attention onto the E//c axis emission from Yb:YLF in this study, as it is around 2 times stronger than the E//a emission and has sharper emission lines. However, un-polarized (E//c + E//a) or E//a emission of Yb:YLF could also be used for temperature estimation, at the expense of a slightly reduced slope in temperature calibration curves.

Once we have collected temperature dependent reference emission data and prepared the calibration curves, the system is cooled down again by refilling liquid nitrogen, and the crystals are pumped with the pump module operating in continuous wave (cw) regime, where incident cw pump powers up to 850 W were applied to the crystals. The untouched emission setup was used to measure the emission in c-axis at different pump power levels, and the collected data is used in predicting the temperature increase of the Yb:YLF crystals with increasing thermal load.

3. Summary of methods used in temperature probing

Figure 2(a) shows the measured c-axis reference emission spectra of Yb:YLF as a function of temperature for temperature ranges in between 78 K and 300 K in normalized (arbitrary) units. As expected, with increasing phonon energy at elevated temperatures, the emission lines get broader, and the emission spectra gets smoother. Figure 2(b) shows the spectral change near the 995 nm region where the measured variation with temperature is largest. As one can see, with increasing temperature the sharp emission peak around 992.4 nm and 995 nm widens out with heating (points 1 and 2 in the figure). Moreover, the spectral dip (around 993.5 nm, point 3 in the figure) between these peaks fills in slowly and even disappears at temperatures above 250 K.

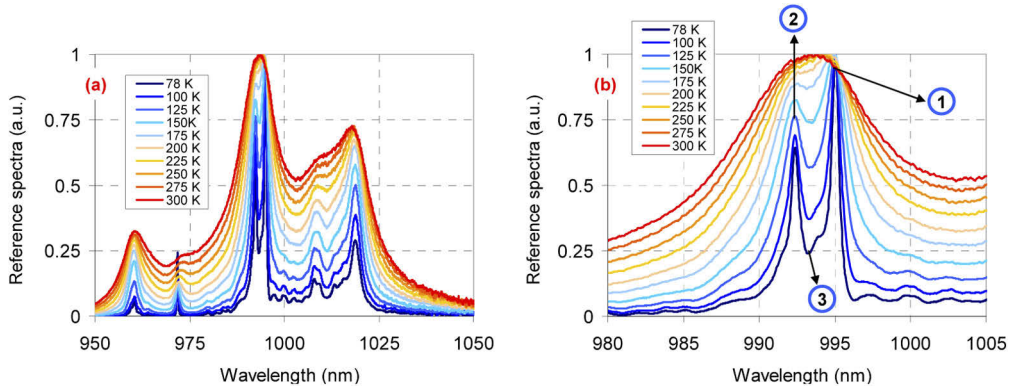

Fig. 2. (a) Measured normalized reference emission spectra of 0.5%-doped Yb:YLF in the c-axis as a function of temperature for temperatures in the range from 78 K to 300 K. (b) A closer look at temperature induced changes in emission spectra in the 980-1005 nm wavelength range.

It is clear that the measured spectral change in emission could be used for estimation of the temperature. For that purpose we have tried the following methods:

Optical Materials EXPRESS

- Peak method: In this method we have used the temperature dependence of the ratio of the intensity around 992.4 nm to the intensity around 995 nm (ratio of intensity of point 2 to point 1). Note that, in the normalized spectra, the intensity around 995 nm is 1. However, for highly doped samples, due to self-absorption effect, the peak of the measured emission might shift to around 1018 nm, so the intensity of the 995 nm peak is not necessarily 1.
- Dip method: Temperature dependence of the ratio of the intensity around the 993.5 nm dip to the intensity around 995 nm peak was utilized (ratio of intensity around point 3 to point 1).
- FWHM method: We have considered the temperature dependence of the full-width half-maximum of the transition (the total spectral width of the 992.4 nm and 995 nm emission is considered).
- DLT method: We have used the overall change in spectra in the whole emission band, as it will be detailed below.

Figure 3 shows the measured variation of the above mentioned quantities with temperature for the 0.5% and 1% doped Yb:YLF samples (could also be named as temperature calibration curves). Here, two independent sets of measurements were done for different doping levels, because as it is well known, the emission measured from Yb:YLF is heavily affected due to the existence of overlapping absorption bands. Hence, as shortly mentioned above, the measured reference emission spectra and the variation of the FWHM and peak ratios might vary with the doping of the crystal used, and also with the position of the excitation beam with respect to crystal, and even with the size of the probe beam used. As a result, a very thin and lowly doped sample is preferred for accurate determination of emission cross section. On the other hand, for this work, where the specific aim is to accurately estimate the temperature of laser crystals under thermal load, we have collected the reference data with Yb:YLF crystals with doping adequate for lasing and the emission collection geometry is chosen to be exactly same as the one that is used in laser experiments. In general, the reference spectrum should be collected very carefully, in a geometry similar to the intended use of Yb:YLF sample to minimize temperature estimation errors. In our measurements, we have chosen the same pump beam size and pump beam position (as seen in Fig. 1(b)), and the different doping of the samples still created an observable shift in spectral properties. It is clear from Fig. 3 that, in general, with increasing temperature, the FWHM of the line increases and as the spectra gets smoother, the strength of dips and peaks diminish, and one gets a flatter spectrum (intensity ratios tend to 1 as temperature increases).

Figure 3(b) also shows the measured variation of integrated overall absolute spectral change with temperature (the calibration curve for the differential luminescence thermometry method). As mentioned earlier, the DLT method is already used in estimating the temperature of Yb:YLF samples in cryogenic optical refrigeration experiments [21–24], but to the best of our knowledge, its capabilities and error margins of temperature estimation for Yb:YLF have not been yet reported. In the DLT method, one calculates the spectral change at different wavelengths with respect to a reference spectrum at a chosen temperature. The reference temperature is taken as 78 K in our case. Figure 4 shows the calculated spectral change ($\Delta S(\lambda, T, T_0)$) with respect to the measured 78 K spectrum ($T_0 = 78\ K$). For the DLT calculations, the spectrum is normalized to prevent intensity fluctuations using [23]:

$$\Delta S(\lambda, T, T_0) = \frac{S(\lambda, T)}{\int S(\lambda, T) d\lambda} - \frac{S(\lambda, T_0)}{\int S(\lambda, T_0) d\lambda}, \tag{1}$$

where T is the temperature, λ is again the wavelength, $S(\lambda, T)$ is the measured emission spectra at different temperatures and the integration limit covers the whole emission range of Yb:YLF

Optical Materials EXPRESS

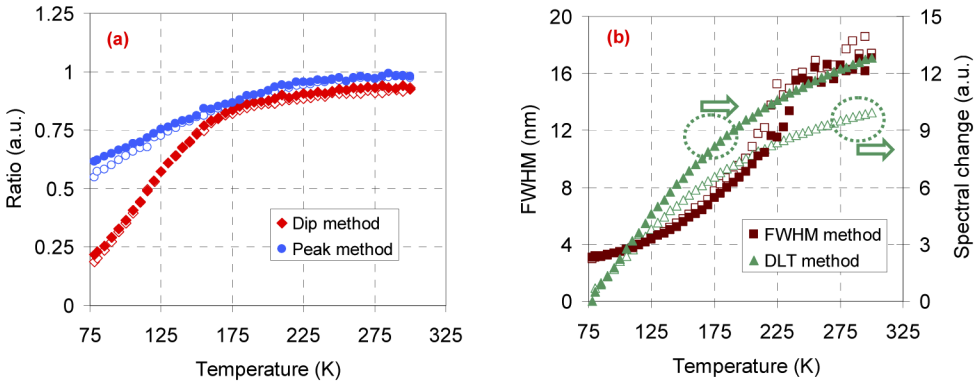

Fig. 3. (a) Measured variation of ratio of the intensity of 992.4 nm peak to the intensity of 995 nm peak (peak method), and the ratio of the intensity of the 993.5 nm dip to the intensity of 995 nm peak (dip method) with temperature. (b) Measured variation of the total FWHM of the 992.4 nm and 995 nm peaks with temperature (FWHM method). The calculated variation of integrated absolute change in spectral shape is also shown (DLT method), where the 78 K spectrum is used as a baseline. The measurements were performed for 0.5 and 1% Yb-doped YLF samples. Empty markers shows the data of 1% Yb:YLF, whereas filled in markers represent the 0.5% Yb:YLF data.

(limited to 950-1025 nm region in this study). Note that, the calculated integrated spectral change shown earlier in Fig. 3(b) is the absolute area of the differential spectrum:

$$S_{DLT}(T, T_0) = \int |\Delta S(\lambda, T, T_0)| d\lambda. \tag{2}$$

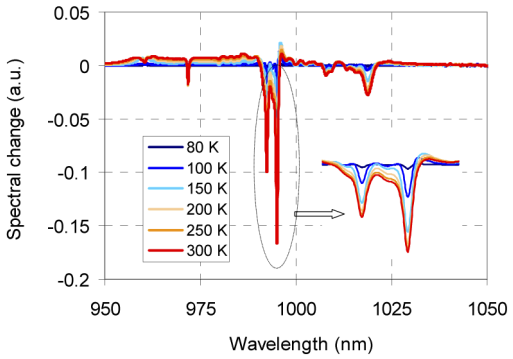

Fig. 4. Calculated spectral intensity change ($\Delta S(\lambda, T, T_0)$, Eq. (1) in the c axis of Yb:YLF, compared to a reference spectrum taken at a temperature of 78 K ($T_0 = 78\ K$).

As it is clear from Fig. 3(b), there is a significant difference between the calculated DLT signal calibration curve for the 0.5% and 1% doped YLF crystals, which shows the large sensitivity of the method to emission collection geometry and crystal specifications, and this calls for utter attention while taking the reference data. Note, that the variation of calibration curves with doping is not as strong in other methods, but to achieve the greatest accuracy in temperature estimation, care should be taken in all cases.

Optical Materials EXPRESS

4. Analysis and comparison of prediction accuracy for different methods

In this section, we will analyze the accuracy of the different methods in predicting the temperature of Yb:YLF crystals. For that purpose, we have measured the temperature dependent emission spectra of Yb:YLF at more than 500 temperatures between 78 K and 300 K. As described earlier, some of this data is used to obtain the calibration curves for different methods (Fig. 3). We have randomly used some of the remaining data to investigate the temperature estimation accuracy of different methods. For this purpose, Fig. 5 shows the measured (measured by the semiconductor sensor in the heat sink) and estimated temperatures for the 0.5 and 1% Yb-doped samples in the 78-300 K temperature range. Similarly, Fig. 6 shows the error in temperature estimation for the different methods. Here we define error as the difference between the estimated and measured temperatures. As mentioned earlier, the dip, peak and FWHM methods are not expected to produce accurate results above 150 K, since the structures providing the temperature information mostly disappear at these temperatures. Their results are still included in all temperature ranges for the sake of completeness.

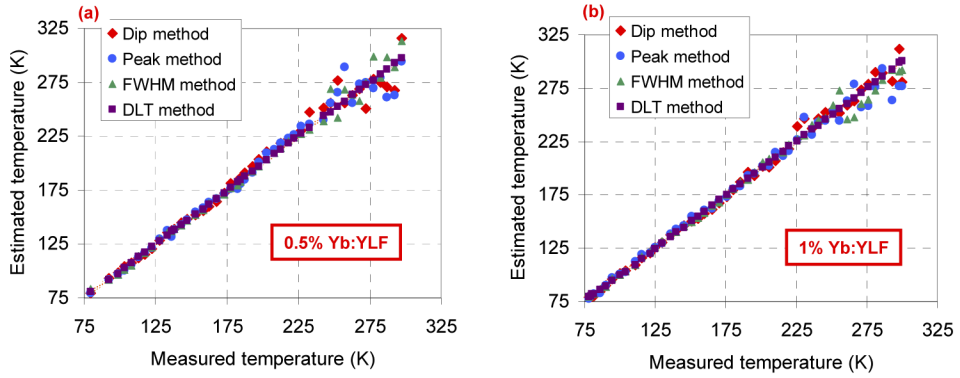

Fig. 5. Measured and estimated temperature of Yb:YLF using different methods for the (a) 0.5% and (b) 1% Yb-doped YLF crystals.

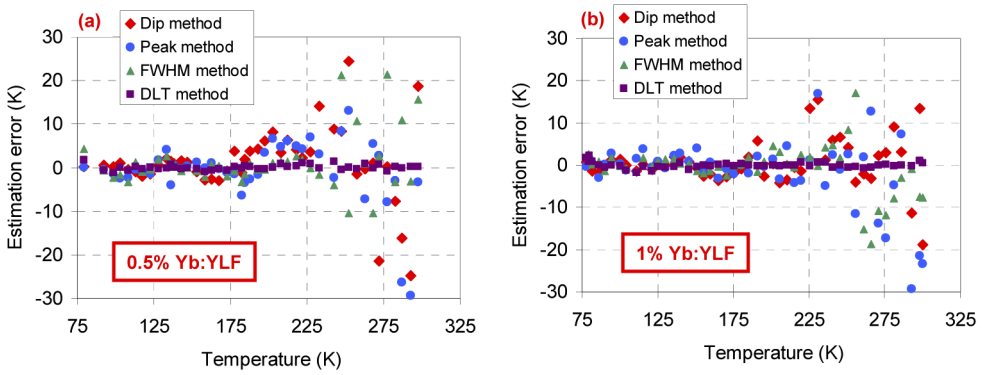

Fig. 6. Calculated estimation error in Yb:YLF crystal temperature prediction using different methods for the (a) 0.5% and (b) 1% Yb-doped YLF crystals.

The result of the estimation accuracy analysis is also summarized in Table 1, where we have listed standard deviation (SD) of the temperature estimation errors for different methods. The table shows estimation error bars in different temperature ranges: 78-100 K, 100-150 K, 150-200 K, 200-250 K, 250-300 K, 78-200 K, and 78-300K. Table 1 also shows the data for the 0.5 and 1%

Optical Materials EXPRESS

doped Yb:YLF separately. When we look at the whole temperature range (78-300 K), the DLT method which can be used to estimate temperatures with average temperature estimation accuracy better than ±1 K stands out as the best option out of the four techniques that is analyzed here. Note on the other hand that, for small temperature differences (78-100 K range), the temperature estimation accuracy of the DLT method is relatively low. This is intrinsic to the nature of the technique, which is affected by the small noise terms, when the ratio of actual signal to noise is small (which is exactly the case for small temperature differences: 78-100 K range). Note, that the absolute sign in Eq. (2) prevents the random noise to cancel each other (plus and minus terms add up), and hence working in a system with a high SNR ratio and dynamic range is useful for the DLT technique. On the other hand, the DLT technique works better and better as the temperature difference increases: the error bars go below ±0.5 K in the 250-300 K range. As a final note on the DLT technique, it is very sensitive to the quality of the reference spectrum $S(\lambda, T_0)$, which is the emission spectrum measured at 78 K (T_0) for our case. As discussed earlier, due to the overlapping absorption and emission bands in Yb:YLF, the reference spectrum shape will depend on many factors such as doping of the crystal, the excitation beam size, the position of the excitation beam within the crystal, the fluorescence imaging geometry, the spectrometer used and the setting of the spectrometer while imaging. Hence, the DLT method works very well if care is taken to have the same conditions of data collection for the reference and temperature measurement spectra. Otherwise, the technique has a DC background, resulting in an overshoot of temperatures.

Table 1. Comparison of temperature estimation accuracy of the different techniques in various temperature intervals. Standard deviation (SD) of errors is given in the table for comparison.

Temperature range (K)	Doping (%)	Dip method error (K)	Peak method error (K)	FWHM method error (K)	DLT method error (K)
78-100	0.5	0.55	1.07	2.97	1.15
	1	1.12	1.65	1.34	0.99
100-150	0.5	1.35	2.15	1.60	0.35
	1	1.14	1.79	1.16	0.62
150-200	0.5	3.78	3.38	1.32	0.42
	1	2.71	2.08	2.04	0.22
200-250	0.5	6.63	3.95	7.97	0.63
	1	6.49	6.11	2.61	0.43
250-300	0.5	15.85	17.77	10.87	0.49
	1	9.06	13.73	10.40	0.48
78-150	0.5	1.20	1.92	1.93	0.67
	1	1.11	1.80	1.29	0.86
78-300	0.5	8.25	8.78	6.25	0.61
	1	5.55	8.11	5.65	0.68

It is clear from Figs. 2 and 3, that other methods of temperature estimation are only expected to work well for temperatures below 150 K. If we look at the estimation error performance in the 78-150 K range, which is the range where the cryogenic laser crystal should ideally stay anyway, the DLT method again provides an error bar better than ±1 K. On the other hand, the other techniques also work relatively well, and a temperature estimation accuracy of ±2 K looks feasible with all the methods. Hence, this shows that, in the lab one can easily estimate the average temperature of the system in real time using any of the peak, dip and FWHM methods within ±5 K accuracy (a ±2 K accuracy should also be feasible for a carefully referenced system).

Optical Materials EXPRESS

It is also interesting to note that, in general, the error bars with the 1%-doped YLF crystal is slightly lower than the 0.5% crystal. We believe this might be due to the higher absorption of the 1% crystal which enables acquisition of fluorescence signals with a higher signal-to-noise ratio. This suggests that for highly doped Yb:YLF samples (such as the 10% samples that are usually used in cryogenic cooling experiments), the error bars of the measurement could be even lower.

5. Temperature measurement of Yb:YLF crystals under thermal load

In this last section, we would like to discuss the usability of the proposed temperature estimation techniques in estimating the average temperature of the Yb:YLF laser crystals under thermal load. In the lab, while working on the cryogenic lasers and amplifiers, one is sometimes not sure about the real thermal state of the crystal. Especially, for materials like Yb:YLF, where the negative dn/dt coefficient is balanced by other positive thermal lens components, and the overall thermal lens is relatively weak, the temperature of the crystal might get too hot, before a significant change of beam profile is observed. Hence, a fast real-time estimation of temperature is desired to prevent accidental overheating of the crystal.

As an example, Fig. 7(a) shows the estimated average temperature of the 0.5% Yb-doped YLF crystal using different techniques at different absorbed pump power levels (when excited with a 2.1 mm diameter 960 nm pump beam). From the earlier analysis we know that, the DLT method gives the best temperature estimate, and as we can see from the data in Fig. 7(a), the temperature estimation with the DLT method is mostly on a linear line, and has the least deviation. The other methods deviate more, but within ±5 K, they also provide the same temperature information. It is important to note here that the temperature profile inside the Yb:YLF crystal is of course position dependent due to one side pumping. Pump saturation effect helps to smooth the temperature profile partially, but numerical simulations show that, temperature differences up to ~10 K could still be present at 300-400W absorbed pump power level (e.g. see Fig. 6 in [31]). In this initial work, we aimed to measure the average temperature of the crystal for a rough estimate of crystals thermal status. Hence, in our measurements the spectrometer input was positioned towards the center of the crystal, where the reference spectra were also collected. A more detailed system, such as what is used for Yb:YAG in [29], is required for a 3-D temperature profile estimation. We believe, that the larger fluctuations observed in Fig. 7(a) for temperature estimation using the

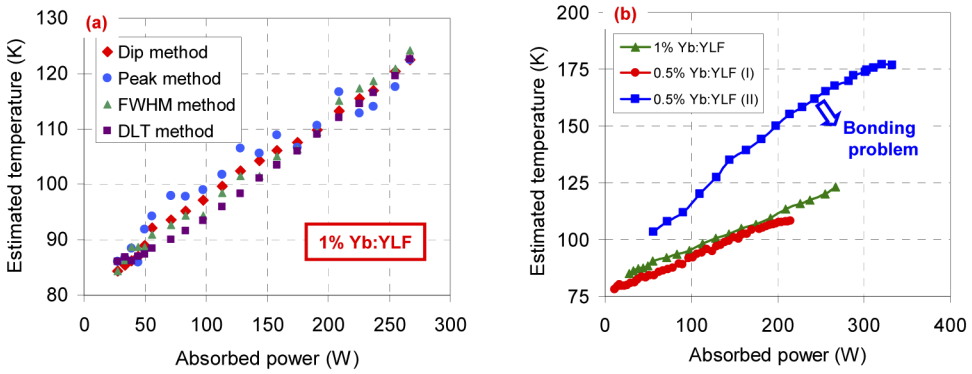

Fig. 7. (a) Estimated average temperature of 1% Yb-doped YLF crystal as a function of absorbed pump power using four different temperature estimation methods. (b) Estimated temperature of two 0.5% and one 1% Yb-doped Yb:YLF crystal as a function of absorbed pump power. One of the 0.5%-doped crystals (crystal II) has a problem in indium bonding resulting in inefficient cooling and fast heating of the crystal. The emission spectra were collected from the central portion of the crystals to achieve an average temperature estimate.

Optical Materials EXPRESS

peak and dip methods might be due to the averaging mechanism of the measurement. Despite the error bars, it is clear that these methods provide very important real-time temperature information to the laser scientist with ±5 K accuracy, and the DLT method could always be used to improve the accuracy for more demanding measurements.

As an example, Fig. 7(b) shows the temperature estimation measurement for three different Yb:YLF crystals: 2 with 0.5%-doping and one with 1% doping. It is clearly visible form the heating curves, that one of 0.5%-doped Yb:YLF crystals has a bad thermal contact (probably a bad bonding) and the crystal is not suitable for laser/amplifier experiments, as it heats up very fast. For the other crystals with a proper thermal contact, the temperature increase is around 0.15 K/W per absorbed pump power, and as an example the 1%-doped YLF crystal reaches a temperature of around 95 K, 110 K and 125 K, at absorbed pump power levels of 100, 200 and 300 W, respectively. Note that the temperature measurements match the temperature estimates in our thermomechanical simulations relatively well [31]. These measurements confirm the benefits of real-time temperature measurements in cryogenic Yb:YLF, as it is very difficult to pinpoint the issues with the laser performance during the experiments, and clearly a fast temperature measurement minimizes the time needed for understanding the problem and/or prevents overheating damage to the crystal.

6. Conclusions

In conclusion, we have presented different methods for temperature estimation of Yb:YLF with accuracy better than ±2K in the 78-150 K range. This is a first step forward in understanding the different contributions of thermal lensing in cryogenic Yb:YLF lasers/amplifiers. Our future work will focus on measuring the different contributions of thermal lensing in Yb:YLF, where we hope to determine the polarizability difference parameter and the photoelastic parameters. Hopefully, a better understanding of the thermal issues will help the laser community to design even higher power cryogenic Yb:YLF systems in the coming decades.

Funding

European Research Council (609920).

Acknowledgements

The authors acknowledge support from previous group members L. E. Zapata, K. Zapata for establishing the indium-bonding technology for YLF at CFEL-DESY. UD acknowledges support from BAGEP Award of the Bilim Akademisi.

Disclosures

The authors declare no conflicts of interest.

References

1. J. Kawanaka, H. Nishioka, N. Inoue, and K. Ueda, "Tunable continuous-wave Yb : YLF laser operation with a diode-pumped chirped-pulse amplification system," Appl. Opt. **40**(21), 3542–3546 (2001).
2. D. Alderighi, A. Pirri, G. Toci, and M. Vannini, "Tunability enhancement of Yb:YLF based laser," Opt. Express **18**(3), 2236–2241 (2010).
3. N. Coluccelli, G. Galzerano, L. Bonelli, A. Di Lieto, M. Tonelli, and P. Laporta, "Diode-pumped passively mode-locked Yb : YLF laser," Opt. Express **16**(5), 2922–2927 (2008).
4. F. Pirzio, L. Fregnani, A. Volpi, A. Di Lieto, M. Tonelli, and A. Agnesi, "87 fs pulse generation in a diode-pumped semiconductor saturable absorber mirror mode-locked Yb:YLF laser," Appl. Opt. **55**(16), 4414–4417 (2016).
5. M. Vannini, G. Toci, D. Alderighi, D. Parisi, F. Cornacchia, and M. Tonelli, "High efficiency room temperature laser emission in heavily doped Yb : YLF," Opt. Express **15**(13), 7994–8002 (2007).
6. W. Bolanos, F. Starecki, A. Braud, J. L. Doualan, R. Moncorge, and P. Camy, "2.8 W end-pumped Yb^{3+}:$LiYF_4$ waveguide laser," Opt. Lett. **38**(24), 5377–5380 (2013).

Optical Materials EXPRESS

7. K. Beil, S. T. Fredrich-Thornton, C. Kränkel, K. Petermann, D. Parisi, M. Tonelli, and G. Huber, "New thin disk laser materials: Yb:ScYLO and Yb:YLF," in *Conference on Lasers and Electro-Optics Europe* (IEEE, 2011).
8. J. Kawanaka, K. Yamakawa, H. Nishioka, and K. Ueda, "Improved high-field laser characteristics of a diode-pumped Yb:$LiYF_4$ crystal at low temperature," Opt. Express **10**(10), 455–460 (2002).
9. J. Kawanaka, S. Tokita, H. Nishioka, M. Fujita, K. Yamakawa, K. Ueda, and Y. Izawa, "Dramatically improved laser characteristics of diode-pumped Yb-doped materials at low temperature," Laser Phys. **15**, 1306–1312 (2005).
10. D. Rand, D. Miller, D. J. Ripin, and T. Y. Fan, "Cryogenic Yb^{3+}-doped materials for pulsed solid-state laser applications [Invited]," Opt. Mater. Express **1**(3), 434–450 (2011).
11. R. L. Aggarwal, D. J. Ripin, J. R. Ochoa, and T. Y. Fan, "Measurement of thermo-optic properties of $Y_3Al_5O_{12}$, $Lu_3Al_5O1_2$, $YAIO_3$, $LiYF_4$, $LiLuF_4$, BaY_2F_8, $KGd(WO_4)_2$, and $KY(WO_4)_2$ laser crystals in the 80-300 K temperature range," J. Appl. Phys. **98**(10), 103514 (2005).
12. L. E. Zapata, D. J. Ripin, and T. Y. Fan, "Power scaling of cryogenic Yb:LiYF4 lasers," Opt. Lett. **35**(11), 1854–1856 (2010).
13. U. Demirbas, H. Cankaya, J. Thesinga, F. X. Kartner, and M. Pergament, "Efficient, diode-pumped, high-power (>300W) cryogenic Yb:YLF laser with broad-tunability (995-1020.5 nm): investigation of E//a-axis for lasing," Opt. Express **27**(25), 36562–36579 (2019).
14. U. Demirbas, H. Cankaya, Y. Hua, J. Thesinga, M. Pergament, and F. X. Kaertner, "20-mJ, sub-ps pulses at up to 70 W average power from a cryogenic Yb:YLF regenerative amplifier," Opt. Express **28**(2), 2466–2479 (2020).
15. D. E. Miller, L. E. Zapata, D. J. Ripin, and T. Y. Fan, "Sub-picosecond pulses at 100 W average power from a Yb:YLF chirped-pulse amplification system," Opt. Lett. **37**(13), 2700–2702 (2012).
16. U. Demirbas, J. Thesinga, H. Cankaya, M. Kellert, F. X. Kartner, and M. Pergament, "High-power passively mode-locked cryogenic Yb:YLF laser," Opt. Lett. **45**(7), 2050–2053 (2020).
17. V. Pilla, P. R. Impinnisi, and T. Catunda, "Measurement of saturation intensities in ion doped solids by transient nonlinear refraction," Appl. Phys. Lett. **70**(7), 817–819 (1997).
18. V. V. Zelenogorskii and E. A. Khazanov, "Influence of the photoelastic effect on the thermal lens in a YLF crystal," Quantum Electron. **40**(1), 40–44 (2010).
19. O. Slezak, A. Lucianetti, M. Divoky, M. Sawicka, and T. Mocek, "Optimization of wavefront distortions and thermal-stress induced birefringence in a cryogenically-cooled multislab laser amplifier," IEEE J. Quantum Electron. **49**(11), 960–966 (2013).
20. Z. L. Zhang, Q. Liu, M. M. Nie, E. C. Ji, and M. L. Gong, "Experimental and theoretical study of the weak and asymmetrical thermal lens effect of Nd:YLF crystal for sigma and pi polarizations," Appl. Phys. B **120**(4), 689–696 (2015).
21. S. Melgaard, "*Cryogenic optical refrigeration: Laser cooling of solids below 123 K*," (University of New Mexico, 2013).
22. S. D. Melgaard, A. R. Albrecht, M. P. Hehlen, and M. Sheik-Bahae, "Solid-state optical refrigeration to sub-100 Kelvin regime," Sci. Rep. **6**(1), 20380 (2016).
23. D. V. Seletskiy, S. D. Melgaard, S. Bigotta, A. Di Lieto, M. Tonelli, and M. Sheik-Bahae, "Laser cooling of solids to cryogenic temperatures," Nat. Photonics **4**(3), 161–164 (2010).
24. S. Melgaard, D. Seletskiy, V. Polyak, Y. Asmerom, and M. Sheik-Bahae, "Identification of parasitic losses in Yb:YLF and prospects for optical refrigeration down to 80 K," Opt. Express **22**(7), 7756–7764 (2014).
25. A. Pant, X. J. Xia, E. J. Davis, and P. J. Pauzauskie, "Solid-state laser refrigeration of a composite semiconductor Yb:$YLiF_4$ optomechanical resonator," Nat. Commun. **11**(1), 3235 (2020).
26. A. Di Lieto, A. Sottile, A. Volpi, Z. H. Zhang, D. V. Seletskiy, and M. Tonelli, "Influence of other rare earth ions on the optical refrigeration efficiency in Yb:YLF crystals," Opt. Express **22**(23), 28572–28583 (2014).
27. A. Volpi, A. Di Lieto, and M. Tonelli, "Novel approach for solid state cryocoolers," Opt. Express **23**(7), 8216–8226 (2015).
28. H. Furuse, J. Kawanaka, N. Miyanaga, H. Chosrowjan, M. Fujita, K. Takeshita, and Y. Izawa, "Output characteristics of high power cryogenic Yb:YAG TRAM laser oscillator," Opt. Express **20**(19), 21739–21748 (2012).
29. H. Chi, K. A. Dehne, C. M. Baumgarten, H. C. Wang, L. Yin, B. A. Reagan, and J. J. Rocca, "In situ 3-D temperature mapping of high average power cryogenic laser amplifiers," Opt. Express **26**(5), 5240–5252 (2018).
30. H. Burton, C. Debardelaben, W. Amir, and T. A. Planchon, "Temperature dependence of Ti:Sapphire fluorescence spectra for the design of cryogenic cooled Ti:Sapphire CPA laser," Opt. Express **25**(6), 6954–6962 (2017).
31. U. Demirbas, H. Cankaya, J. Thesinga, F. X. Kärtner, and M. Pergament, "Power and energy scaling of rod-type cryogenic Yb:YLF regenerative amplifiers," J. Opt. Soc. Am. B **37**(6), 1865–1877 (2020).

217.93.243.88 (to 2020-12-01 14:42:21)